Quantum communication and memory with entangled atomic ensembles

Eugene Polzik, Brian Julsgaard, Christian Schori and Jens Sørensen
QUANTOP - Danish National Research Foundation Center for Quantum Optics, Department of Physics and Astronomy, University of Aarhus, Denmark

1 Introduction

Quantum information processing, a rapidly developing area of physics, involves operations with quantum states, in which information can be encoded. The number of degrees of freedom available for the encoding grows dramatically, as compared to classical encoding, due to the existence of quantum superpositions.

One of the necessary components for quantum information processing is the quantum state transfer between distant nodes of a quantum network. Light is a natural agent for such a transfer, whereas atoms are natural agents for storing the information. Therefore, a problem of efficient quantum state interface between light and atoms has become one of the major problems in the field. Conceptually the simplest scenario for such an exchange involves an interaction of a single photon (a flying qubit) with a single atom (a stationary qubit). However, efficient interaction of this kind requires the atom and the photon be coupled to a high finesse cavity [1,2]. Although spectacular results have been achieved along these lines, the quantum interface between the flying and stationary qubits remains a challenge.

Several years ago we have initiated a new approach to this problem involving atomic ensembles and multi-photon states. In the first attempt [3] the transfer of a squeezed state of light onto a spin squeezed state of a cold atomic sample via complete absorption of light has been demonstrated. Further theoretical development which makes use of Raman processes followed [4].

However, an off-resonant type of interaction as suggested in [5,6] proved to be more versatile and promising for the quantum interface. This interaction, which has been earlier used for detecting quantum noise of atomic states [7,3] and for generation of spin squeezed atomic state via a quantum nondemolition measurement [8] is the basis for the experiments discussed in this paper.

2 Collective continuous quantum variables for light and atomic ensembles

In case of multi-atom ensembles and multi-photon pulses collective atomic spin and quantized Stokes parameters of light are used as quantum variables. Fig.1 illustrates two non-commuting transverse components of the spin, J_z, J_y of an ensemble polarized along the *x*-axis. The spin components obey the usual commutation relations, from which the uncertainty relation follows:

$$\left[\hat{J}_y, \hat{J}_z\right] = i\hat{J}_x \Rightarrow \delta J_y \delta J_z \geq \tfrac{1}{2} J_x = \tfrac{1}{4} N \qquad (1)$$

For independent atoms, which form a coherent spin state, the two uncertainties are equal. Unless specified otherwise we will discuss the simple case of spin ½ atoms.

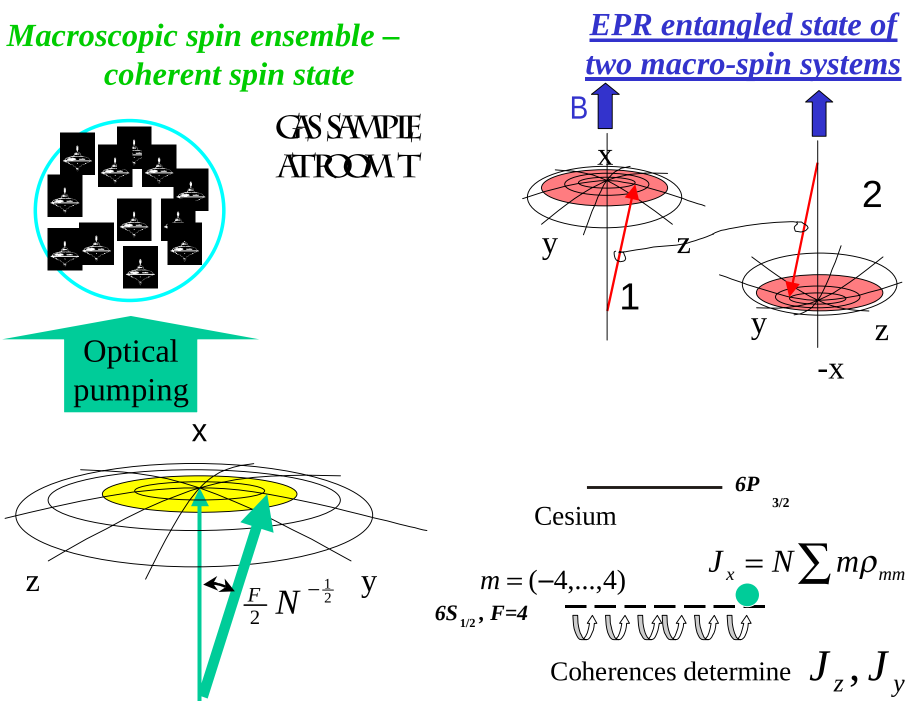

Figure 1: Collective spin states of multi-atoms samples.

When non-interacting atoms are optically pumped along the direction x, a coherent spin state is generated. The transverse components of the collective spin z and y cannot be defined simultaneously to better than the quantum uncertainty. Two entangled atomic samples have their spins parallel to the precision better than this quantum uncertainty. In the experiments the spin state of the ground state Cesium atoms has been used.

Entangled states of distant atomic objects are required for atomic teleportation and quantum networking. Using atomic ensembles we have recently generated the entangled state of two Cs cells by sending a pulse of light through them and performing a projection measurement of polarization of the light, as described in the next Section. For two atomic collective spins, such as shown in Fig. 1, the necessary and sufficient entanglement condition can be derived from the results of [9]:

$$\left\langle \left(\hat{J}_{z1} + \hat{J}_{z2}\right)^2 \right\rangle + \left\langle \left(\hat{J}_{y1} + \hat{J}_{y2}\right)^2 \right\rangle < 2J_x \tag{2}$$

Since the operators of the sum of two z projections and the sum of the two y projections for two oppositely oriented spin samples commute, the two sums can be measured simultaneously with arbitrary accuracy. Therefore, the variances on the left hand side of the above inequality can be, in principle, made as small as possible. Hence the required entangled state can be generated by a measurement.

3 Generation of the entangled state of two atomic objects

To describe the measurement required for generation of the entanglement of atoms, we need a quantum description of light. A polarized pulse of light is described by Stokes operators obeying the same commutation relation as spin operators, $\left[\hat{S}_y, \hat{S}_z\right] = i\hat{S}_x$. $\hat{S}_x$ is the difference between photon numbers in x and y linear polarizations, $\hat{S}_y$ is the difference between polarizations at $\pm 45^0$, and $\hat{S}_z$ is the difference between the left- and right-hand circular polarizations along the propagation direction, z. In our experiment light is linearly polarized along the x axis. Hence the two pairs of continuous quantum variables engaged in the entanglement protocol are $\hat{J}_z$ and $\hat{J}_y$ for atoms, and $\hat{S}_z$ and $\hat{S}_y$ for light.

As shown in [5,6], when an off-resonant pulse is transmitted through two atomic samples with opposite mean spins $J_{x1} = -J_{x2} = J_x$, the light and atomic variables evolve as

$$\hat{S}_y^{out} = \hat{S}_y^{in} + \alpha\hat{J}_{z12}, \hat{S}_z^{out} = \hat{S}_z^{in}$$
$$\hat{J}_{y1}^{out} = \hat{J}_{y1}^{in} + \beta\hat{S}_z^{in}, \hat{J}_{y2}^{out} = \hat{J}_{y2}^{in} - \beta\hat{S}_z^{in}, \hat{J}_{z1}^{out} = \hat{J}_{z1}^{in}, \hat{J}_{z2}^{out} = \hat{J}_{z2}^{in} \tag{3}$$

The first line describes the Faraday effect (polarization rotation of the probe). The second line shows the back action of light on atoms, i. e., spin rotation due to the angular momentum of light. According to (3), the measurement of $\hat{S}_y^{out}$ reveals the value of $\hat{J}_{z12} = \hat{J}_{z1} + \hat{J}_{z2}$ (provided the constant α is large enough, so that $\hat{S}_y^{in}$ is relatively small) without changing this value. It follows from (3) that the total y spin projection for both samples is also conserved, $\hat{J}_{y1}^{out} + \hat{J}_{y2}^{out} = \hat{J}_{y1}^{in} + \hat{J}_{y2}^{in}$. The procedure can be repeated with another pulse of light measuring the sum of y components, $\hat{J}_{y1} + \hat{J}_{y2}$, again in a non-demolition way, while at the same time leaving the previously measured value of $\hat{J}_{z1} + \hat{J}_{z2}$ intact. As a result, the sum of the z components and the sum of the y components of spins of the two samples are known exactly in the ideal case, and therefore the two samples are entangled.

Instead of making two consecutive measurements of y and z projections, we place the samples in a magnetic field oriented along the direction of spin orientation. The Larmor precession of the J_z, J_y components with a common frequency Ω does not change their mutual orientation and size and therefore does not affect the entanglement. On the other hand, the precession allows us to extract information about both z and y components from a single probe pulse. Moreover, in the lab frame the spin state is now encoded at the frequency Ω, and as usual an ac measurement is easier to reduce to the quantum noise level than a dc measurement. Measurements of the light noise can be now conducted only around its Ω spectral component. By choosing a suitable radio-frequency value for Ω we can reduce the probe noise $\hat{S}_{y,z}^{in}(\Omega)$ to the minimal level of the vacuum (shot) noise.

In the presence of the magnetic field the spin behavior is described by the following equations: $\dot{\hat{J}}_z(t) = \Omega \hat{J}_y(t), \dot{\hat{J}}_y(t) = -\Omega \hat{J}_z(t) + \beta \hat{S}_z(t)$. Solving the spin equations and using (3) we obtain

$$\hat{S}_y^{out}(t) = \hat{S}_y^{in}(t) + \alpha \left\{ \hat{J}_{z12} \cos(\Omega t) + \hat{J}_{y12} \sin(\Omega t) \right\} \qquad (4)$$

The $\hat{J}_{z,y}$ components are now defined in the frame rotating with the frequency Ω around the magnetic field direction x. It is clear that by measuring the $\cos(\Omega t)/\sin(\Omega t)$ component of $\hat{S}_y^{out}(t)$ one acquires the knowledge of the z/y spin projections.

The experiment described in detail in [10] has been conducted with two paraffin coated cells filled with Cs around room temperature. Atoms in two cells are oriented in the opposite directions by suitable optical pumping. Then the entangling pulse of light is sent through both cells and quadrature phase components of its polarization around the Larmor frequency are detected by two lock-in amplifiers. After 0.5 msec delay another, verifying, pulse is sent. The difference of the outputs of the two lock-in amplifiers for the two pulses is recorded and its variance computed. For perfect entanglement generated by the first pulse, this variance would be zero. For imperfect, but still entangled state, the variance should be less than that for a single measurement performed on a coherent spin state. The results demonstrating entangled state of two macroscopic atomic objects are shown in Fig. 2.

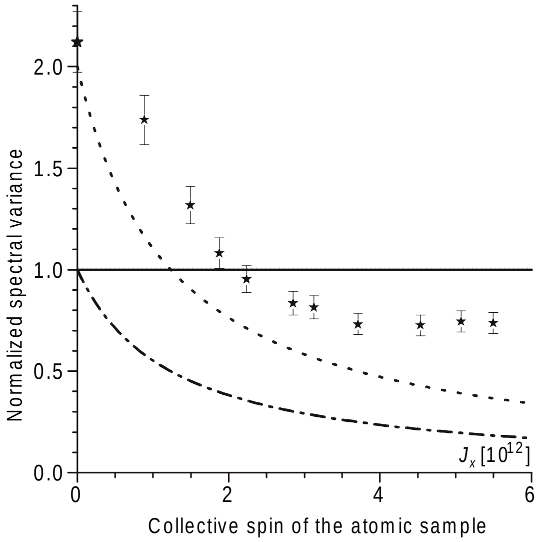

Fig. 2: The variance of the difference between two spin measurements separated in time by 0.5 msec. The variance is normalized to the previously determined value for a single measurement on the sample in a coherent spin state (horizontal line). The experimental points below the line obey the entanglement condition (2). The dotted line corresponds to the best entanglement possible under the experimental conditions. The dash-dotted line represents the quantum noise of the verifying pulse of light without atoms (its dependence on the spin is due to the adopted normalization).

The degree of entanglement calculated from the data in Fig.2 without any additional assumptions reaches $(35 \pm 7)\%$. Taking into account the additional knowledge about initial spin being in the coherent spin state, we obtain, following [6], the degree of entanglement of up to 52%. In both cases the degree of entanglement is defined as one minus the ratio of the left- and right-hand sides of the equation (2).

3. Recording a quantum feature of light in a long lived atomic state.

Another recent example of a quantum interface of free propagating light and an atomic ensemble is the demonstration of the sensitivity of the ground state atomic coherence to the quantum state of light passing through the atomic ensemble [11]. The experimental set-up is similar to the one used for the atomic entanglement described in the previous section, except only one cell has been used. The input could be chosen to be in a vacuum state, i.e., the input is blocked, or in a squeezed vacuum state produced by a narrow-band, frequency tunable source based on a parametric oscillator below threshold [12]. This quantum input has been mixed with a strong classical beam of the same frequency and orthogonal polarization before being sent through atoms. The spectral density $S_y^2(\Omega)$ around the Larmor frequency has been recorded. The resulting spectra for the vacuum and squeezed vacuum inputs are presented in Fig. 3. The spectrum consists of a broadband background due to quantum noise of light and a narrow peak of atomic response. The background is lower for the squeezed vacuum input as expected. However, the narrowband feature corresponding to the atomic memory part is also different for the different inputs, although the difference in terms of the photon flux corresponds to only about 200 photons per second within the bandwidth of the atomic response. This translates into a (few photons/per atomic response time) sensitivity of the spin state of the atomic ensemble.

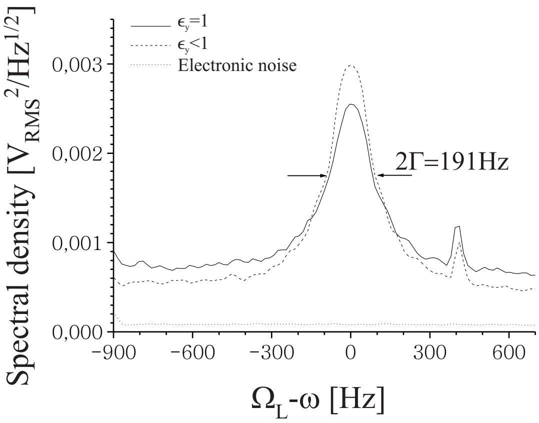

Fig. 3: Recording a quantum feature of light in a long-lived atomic spin state. Spectral density of the photocurrent of the probe light transmitted through an atomic cell. One of the curves corresponds to the vacuum state of light. The other - to the squeezed vacuum state. The width of the resonance indicates the memory time of atoms of 1.5 msec.

Future work will be directed towards recording both quadrature phase components of light in the atomic spin state, which will make it closer to the full scale quantum memory.

4 Protocol for teleportation of an atomic entangled state

The exciting application for the atomic entanglement described in Section 2 is the teleportation of atomic states. Consider four spin polarized cells in the configuration shown in Fig. 4. The left pair of cells belongs to one party, Alice, the right pair belongs to Bob. Several quantum communication protocols can be accomplished with such setting. Via the teleportation procedure entanglement can be generated between cells 1 and 4 despite the fact that they have never interacted with each other. Thus entanglement swapping between cells 2,3 and cells 2,4 can be achieved. Also a secret message encoded in the spin state of cell 2 can be teleported onto the spin state of cell 4. The main steps include sending pulses of light through pairs of cells as shown in the Fig. 4, detecting the pulses polarization states with photodetectors, and rotating the spin of cell 4 according to the results obtained from the detectors.

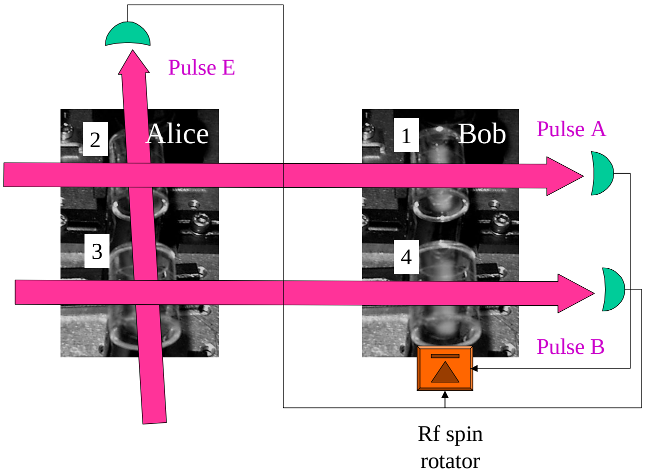

Figure 4: Teleportation of atomic entanglement. Pulses A and B generate shared entanglement between Alice and Bob. Pulse E generates entangled state of Alice's cells 2,3. This entangled state is then teleported onto Bob's cells 1,4 by rotation of the spin 4 according to the classical information from the three detectors.

Magnetic field is oriented perpendicular to the plane of the optical beams and atomic spins are polarized collinear to the direction of the field. Cells 1 and 3 are spin polarized in the direction opposite to the polarization of cells 2 and 4. With such a geometry all the pulses shown in the Fig. 4 interact with oppositely polarized samples, and therefore each of the pulses entangles the pair of cells through which it is sent.

Pulse E is fired after pulses A and B. In the following we assume that the degree of entanglement created by the pulse is large, and omit the initial optical pulse state from the equations. With this assumption the spins of the cells are transformed by optical pulses in a simple way. Detector A measures the value of the y component of the Stokes parameter: $S_A^y = J_1^' + J_2^' = J_1 + J_2$. Each term in this equation, in fact, corresponds to a two-component vector. For the Stokes parameter the two components are the *sin* and *cos* components, whereas for the spins they are the *y* and *z* projections of the spins in the rotating frame, as described in Section 2. The spins of the cells 1 and 2 change according to $J_1^' = J_1 + S_A^z, J_2^' = J_2 - S_A^z$. A similar set of equations is valid for cells 3,4 when the pulse B is fired through these cells, $S_B^y = J_3^' + J_4^' = J_3 + J_4$, $J_3^' = J_3 + S_B^z, J_4^' = J_4 - S_B^z$.

Next, pulse E which entangles cells on Alice's site is fired through cells 2 and 3 and is measured by its detector with the result

$$S_E^y = J_2^{''} + J_3^{''} = J_2^' + j + J_3^' = J_2 + j + J_3 + S_B^z - S_A^z.$$

After all the pulses are fired and their measurements recorded several goals can be achieved.

The two cells, 1 and 4 are entangled because their spins are linked by $J_1^' + J_4^' = S_A^y + S_B^y - S_E^y$. A simple rotation of any of the two spins involved will convert this state into the state $J_1^' + J_4^' = 0$ for which the entanglement is even more evident. This operation is effectively the teleportation of entangled state from Alice to Bob, i.e. the entanglement swapping.

After pulses A and B are detected, but before pulse E is sent, an unknown spin state can be encoded on cell 2 by rotating its spin by a small angle of the order of $N^{-1/2}$. This rotation will not be observable by looking at the spin of the cell 2 alone because its spin state is obscured by the back action of pulse A. If Alice has encoded an unknown spin state *j* in the cell 2, this state can be read by Bob via the rotation of one of his spins by $-S_A^y - S_B^y + S_E^y$ and a joint measurement on his cells to obtain the secret message as follows

$$J_1^' + J_4^' - S_A^y - S_B^y + S_E^y = J_1 + S_A^z + J_4 - S_B^z -$$

$$(J_1 + J_2) - (J_3 + J_4) + J_2 + j + J_3 + S_B^z - S_A^z = j.$$

None of the pulses sent across contains this secret message, nor can it be read by looking at any of the cell taken separately. It requires the full entanglement of the system to be activated for Bob to read the message.

The experimental set-up for the atomic teleportation described above is being constructed and tested. It consists of fours paraffin coated cells $2\times3\times3cm$ each placed in the individual magnetic shield with the coils providing the dc field corresponding to the Larmor frequency about 300 kHz and the rf coils used for performing the spin rotation necessary for the teleportation. The dc field is homogeneous so that the dephasing time of moving atoms is as long as 25 msec (13 Hz linewidth of the magnetic resonance signal). The pumping and entangling pulses are produced in the same way as in [10]. One of the experimental difficulties in [10] was due to the rectangular shape of light pulses in the time domain (the pulses were produced by a mechanical chopper). Such a shape led to spurious ring down noise at the leading and trailing edges of the pulses. This noise limited the time domain over which entanglement could be studied. In the present set-up we use shaping of the pulses with AOMs, producing pulses with smooth shapes, thus eliminating the problem.

5. Conclusions

The paper summarizes recent experimental and theoretical results on developing the quantum interface between propagating light pulses and atomic ensembles [13]. The availability of separate entangled atomic objects and the tunable source of entangled light [11,12] provides us with the toolbox adequate for a number of quantum information processing protocols, including quantum teleportation of atoms, quantum memory for light and multi-partite entanglement generation. The experiments described above are performed with trillions of atoms at room temperature. Smaller and more compact atomic samples can be used provided the required high optical density can be achieved. Natural candidates in this case would be cold and trapped atomic samples, as well as possibly a solid state medium. Although free space atoms allow simpler experiments, placing ensembles in a cavity will provide extra benefits, such as higher efficiency for smaller atomic numbers. According to preliminary calculations, hundreds or thousands of atoms in a bad cavity can be entangled along the lines described in Section 2. Such experiments will belong to an intermediate domain between free space ensembles and single atoms in high-Q cavities.

References

[1] H.J. Briegel, J.I. Cirac, W. Dur, S.J. van Enk, H.J. Kimble, H. Mabuchi, P. Zoller, Lect. Notes in Comp. Science **1509**, 373 (1999)

[2] A. Rauschenbeutel, G. Nogues, S. Osnaghi, P. Bertet, M. Brune, J.M. Raimond, S. Haroche, Science, **288**, 2024 (2000)

[3] A. Kuzmich, K. Molmer, E.S. Polzik, Phys. Rev. Lett., **79**, 4782 (1997); J. Hald, J.L. Sorensen, C. Schori, E.S. Polzik, Phys. Rev. Lett., **83**, 1319 (1999).

[4] A. Kozhekin, K. Molmer, E.S. Polzik, Phys. Rev. A **62**, 033809 (2000)

[5] A. Kuzmich, E.S. Polzik, Phys. Rev. Lett., **85**, 5639 (2000)

[6] L.M. Duan, G. Giedke, J.I. Cirac, P. Zoller, E.S. Polzik, Phys. Rev. Lett., **85**, 5643 (2000)

[7] E.B. Alexandrov, V. Zapassky, J. Exper. Theor. Phys. **81**, 132 (1981)

[8] A. Kuzmich, L. Mandel, N.P. Bigelow, Phys. Rev. Lett., **85**, 1349 (2000)

[9] R. Simon, Phys. Rev. Lett., 84, 2726 (2000); L.M. Duan, G. Giedke, J.I. Cirac, P. Zoller, Phys. Rev. Lett., **84**, 2722 (2000).

[10] B. Julsgaard, A. Kozhekin, E.S. Polzik, Nature, **413**, 400 (2001)

[11] C. Schori, B. Julsgaard, A.L. Sorensen, E.S. Polzik, Phys. Rev.Lett., 89, 057903 (2002).

[12] C. Schori, J. Sorensen, E.S. Polzik, to appear in Phys.Rev. A (2002).

[13] E.S. Polzik, Physics World, September (2002).